TABLE 3 Validation Results

		$y = 1$ m	$y = 2$ m	$y = 3$ m	$y = 4$ m	$y = 5$ m
$z = 0.3$ m	Measured	55.3	57.6	57.8	58.3	58.5
	Radiosity	49.1	53.8	55.2	56.7	57.1
	FDTD	40.4	57.4	47.8	49.9	51.9
$z = 1.0$ m	Measured	52.7	52.7	55.5	56.2	56.5
	Radiosity	49.1	50.4	48.2	53.6	55.9
	FDTD	48.3	43.3	55.5	47.7	47.2
$z = 1.75$ m	Measured	52.4	53.5	54.4	55.6	55.9
	Radiosity	48.3	52.3	50.1	51.9	52.1
	FDTD	38.6	54.3	55.5	51.9	54.1

All values of transmission path loss are in dB

distance), which include both line of sight (LOS) and nonLOS points. The measurements were performed using a virtual multiple input single output (MISO) system setup (Fig. 7). A network analyzer (Agilent Technologies, E5062A 300 kHz–3 GHz ENA Series Network Analyzer) was used to measure the total path loss between the transmitter and the receiver antenna. The channel was probed in a 500 MHz measurement bandwidth at a central frequency of 2.75 GHz. For signal transmission and reception, broadband omnidirectional biconical antennas (Electro-Metrics EM-6116) were used. The network analyzer was connected with these antennas using coaxial cables ($\sim$20 m for the R_X and $\sim$5 m for the T_X) with ferrite sleeves.

Table 3 presents the measured path loss values (dB) at the 15 measurement points together with the calculated values by the radiosity and the FDTD method. The average deviation between measured and calculated by the radiosity method values is -3.27 dB, in contrast to the -6.13 dB average deviation of the FDTD values. The disagreement between measurements and FDTD results can be attributed to the choice of material parameters. It is interesting to note, however, that both software tools predicted a transmission path loss lower than the measured one, which is a conservative approach for coverage studies but not for exposure safety calculations. Another remarkable issue is the computational resources required to derive a full wave solution, compared to those needed by the radiosity method.

5. CONCLUSION

We have presented an implementation of the radiosity method for the calculation of path loss. We have shown that the method can provide a sufficiently accurate prediction of the propagation of the electromagnetic radiation in complex indoor environments. The measurements performed in a real classroom agreed better with the radiosity calculations than with the FDTD results, which required a multifold longer computational time to achieve.

ACKNOWLEDGMENTS

This research has been cofinanced by the European Union (European Social Fund—ESF) and Greek national funds through the Operational Program "Education and Lifelong Learning" of the National Strategic Reference Framework (NSRF)—Research Funding Program: THALES. Investing in knowledge society through the European Social Fund.

REFERENCES

1. T. Kim-Fung, C. Wing-Shing, J. Don, K. Kai, Y. Shiu-Yin, and Z. Wen-Xun, Radiosity method: A new propagation model for microcellular communication, IEEE Antennas Propag Soc Int Symp 4 (1998), 2228–2231.
2. M. Liang and Q. Liu, A practical radiosity method for predicting transmission loss in urban environments, EURASIP J Wirel Commun Networking, 2 (2004), 357–364.
3. M. Ayadi and S. Tabbane, Comparison of radiosity and ray-tracing methods in micro-cellular urban environment, SETIT, 2005.
4. V. Degli-Esposti, F. Fuschini, E.M. Vitucci, and G. Falciasecca, Measurement and modelling of scattering from buildings, IEEE Trans Antennas Propag 55 (2007), 143–153.
5. M.F. Cohen, S.E. Chen, J.R. Wallace, and D.P.Greenberg, A progressive refinement approach to fastradiosity image generation, ACM SIGGRAPH Comput Graphics 22 (1988), 75–84.
6. M.F. Cohen and D.P. Greenberg, The hemi-cube: A radiosity solution for complex environments, ACM SIGGRAPH Comput Graphics 19 (1985), 31–40.
7. E.E. Catmull, A subdivision algorithm for computer display of curved surfaces, University of Utah, Salt Lake City, UT, 1974.
8. A. Muqaibel, A. Safaai-Jazi, A. Bayram, and S.M. Riad, Ultra wideband material characterization for indoor propagation, In: IEEE Antennas and Propagation Society International Symposium, Blacksburg, 2002.

COMPACT DOUBLE BAND-NOTCHED ANTENNA WITH NONEQUIWIDTH W-SHAPED SLOT AND "6"-SHAPED RESONANCE LOOP FOR UWB APPLICATIONS

Tang Yang, Gao Jin Song, Wang Yan Song, and Feng Xiao Guo

Changchun Institute of Optics, Fine Mechanics, and Physics, Changchun, China; Corresponding author: tangyang0816@163.com

Received 2 March 2013

ABSTRACT: *In this article, a novel compact double band-notched antenna with nonequiwidth W-shaped slot and "6"-shaped resonance loop on the two sides of the feed line is proposed, which consists of a cone-shaped monopole patch with nonequiwidth W-shaped slot and "6"-shaped resonance loop on the two sides of the feed line, the metal earth-plate with step slot is designed on other side of the substrate. The simulated and experimental results demonstrate that the proposed antenna can obtain the double band-notched feature within the bandwidth of 3.3–3.8 GHz and 5.0–6.0 GHz, the impedance bandwidth can achieve from 2.4 to 11.6 GHz (VSWR < 2),which is more than 131%.* © 2013 Wiley Periodicals, Inc. Microwave Opt Technol Lett 55:2405–2410, 2013; View this article online at wileyonlinelibrary.com. DOI 10.1002/mop.27859

Key words: *nonequiwidth W-shaped slot; monopole antenna; band-notched; UWB*

1. INTRODUCTION

The ultra-wideband (UWB) technology has developed very quickly since the Federal Communications Commission allocated the frequency range from 3.1 to 10.6 GHz for UWB commercial applications in 2002 [1]. The antennas as one of the most important parts in the whole UWB systems are faced with higher performance demands of easy manufacturing, low cost, simple structure, low profile, broad bandwidth, high gains, and omni-directional radiation patterns. Many planar monopole antennas which meet these demands have been designed for UWB systems in recent years [2–7]. However, the wireless local area network operates in 5.15–5.35 GHz together with 5.725–5.825 GHz and the system of worldwide interoperability for microwave access at 3.4–3.7 GHz bands has been used, to

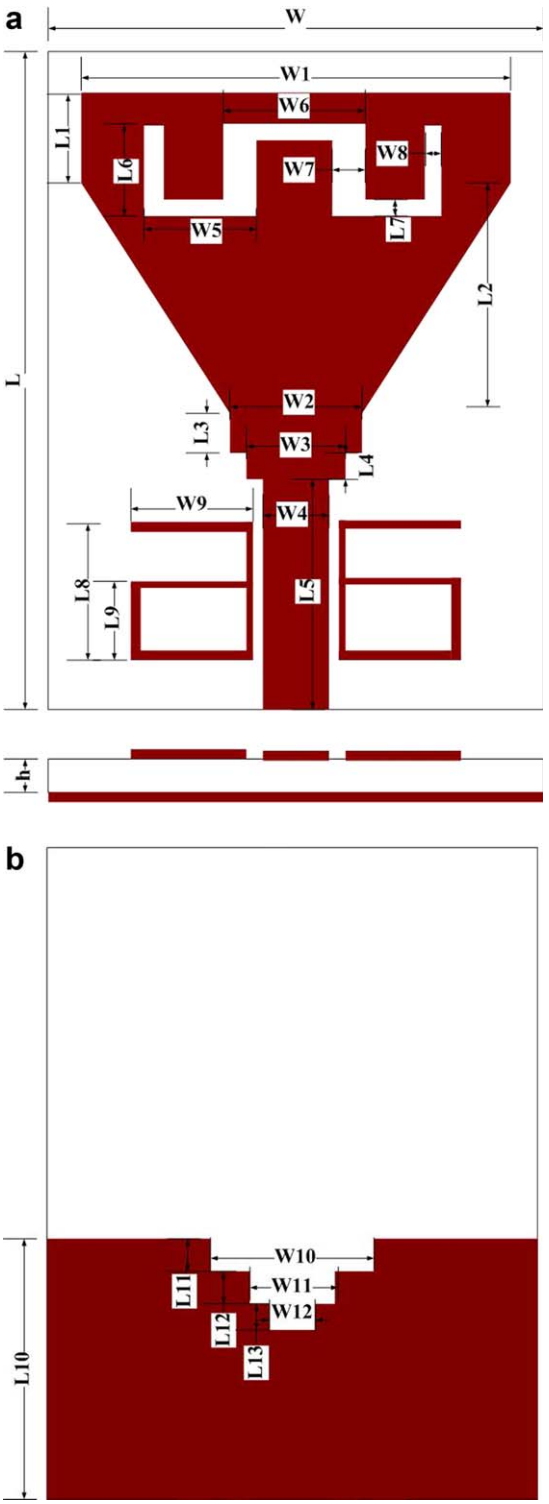

Figure 1 Configuration of the proposed antenna. [Color figure can be viewed in the online issue, which is available at wileyonlinelibrary.com]

reduce the electromagnetic interference between these systems. Lately, some new antennas with band-notched function have been presented for UWB systems which can avoid the interference [8–13].

In this article, a novel compact double band-notched antenna with nonequiwidth W-shaped slot and "6"-shaped resonance loop on the two sides of the feed line is proposed. The 3.3–3.8 GHz band-notched is achieved by drawing into W-shaped slot

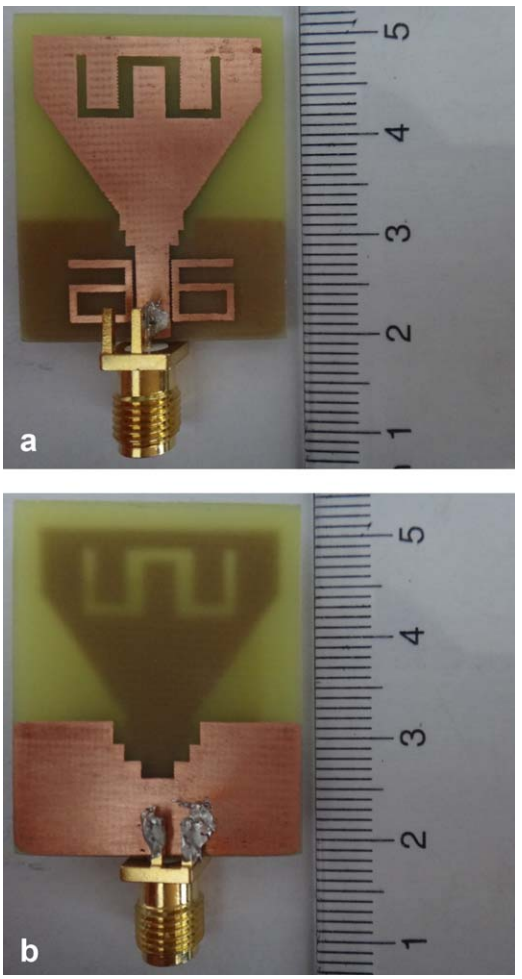

Figure 2 Photograph of the proposed antenna. [Color figure can be viewed in the online issue, which is available at wileyonlinelibrary.com]

in the monopole patch. The 5.0–6.0 GHz band-notched is achieved by drawing into the "6"-shaped resonance loop on the two sides of the feed line.

The simulation and experimental results demonstrate that the antenna can obtain the double band-notched feature within the

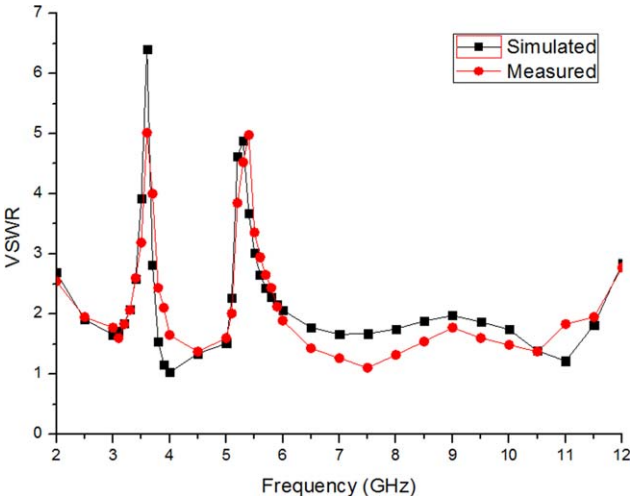

Figure 3 Measured and simulated impedance bandwidth for the proposed antenna. [Color figure can be viewed in the online issue, which is available at wileyonlinelibrary.com]

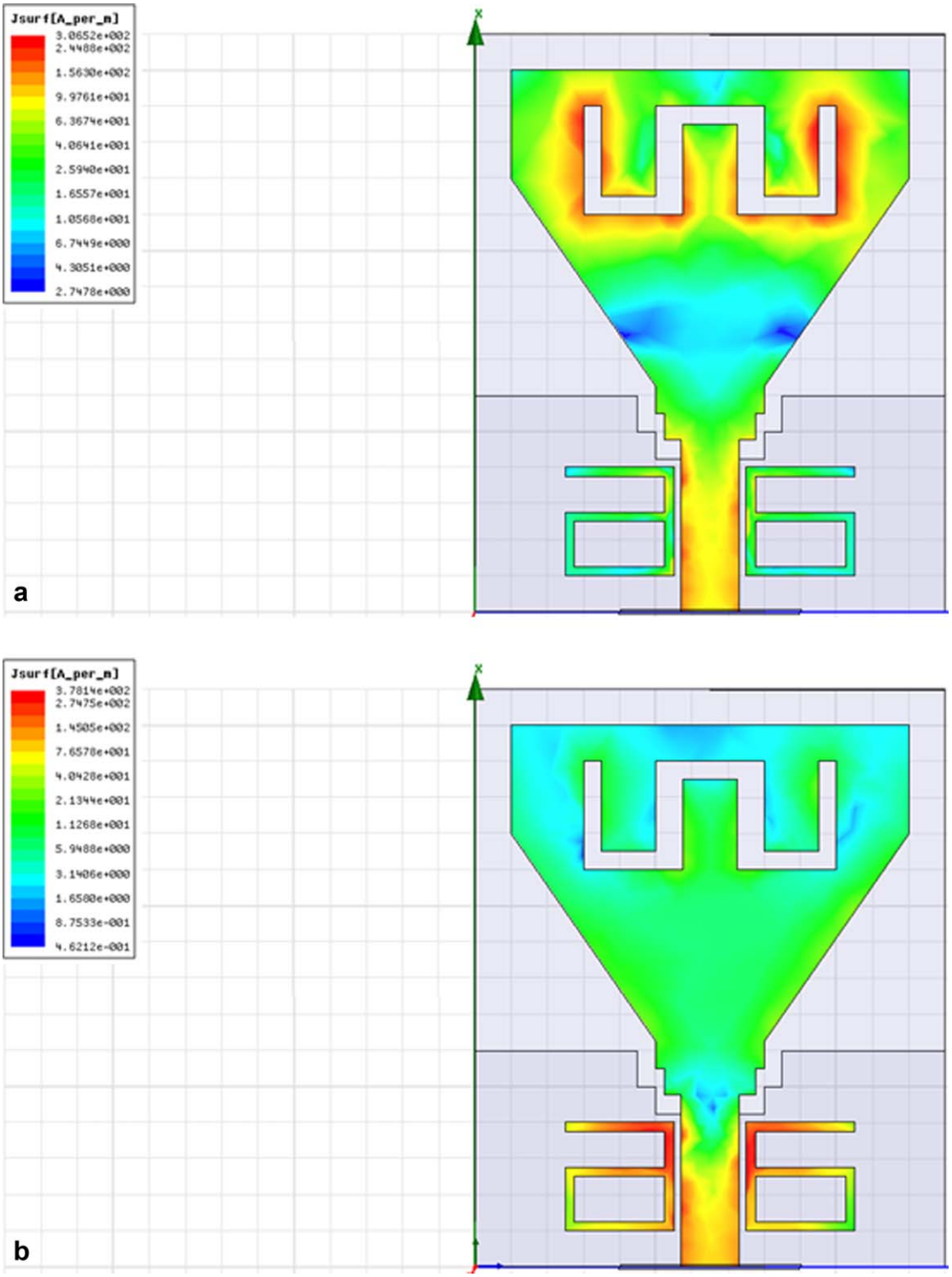

Figure 4 Simulated surface current distribution for the proposed antenna at 3.6 and 5.4 GHz. [Color figure can be viewed in the online issue, which is available at wileyonlinelibrary.com]

bandwidth of 3.3–3.8 GHz and 5.0–6.0 GHz and the impedance bandwidth can achieve from 2.4 to 11.6 GHz (VSWR < 2), which is more than 131%.

2. ANTENNA DESIGN

The configuration of the proposed and fundamental antennas are shown in Figure 1. The substrate of the antenna is FR4 with relative permittivity 4.4, thickness $h = 1.0$ mm, and loss tangent 0.018, the size of the UWB antenna is 26×32 mm^2. The proposed antenna consists of a cone-shaped monopole patch with nonequiwidth W-shaped slot and "6"-shaped resonance loop on the two sides of the feed line, the metal earth-plate with step slot is designed on other side of the substrate and fed by a 50 Ω microstrip feed line which connects to a SMA connector and the width of the feed line is $W4 = 3.2$ mm. The optimized

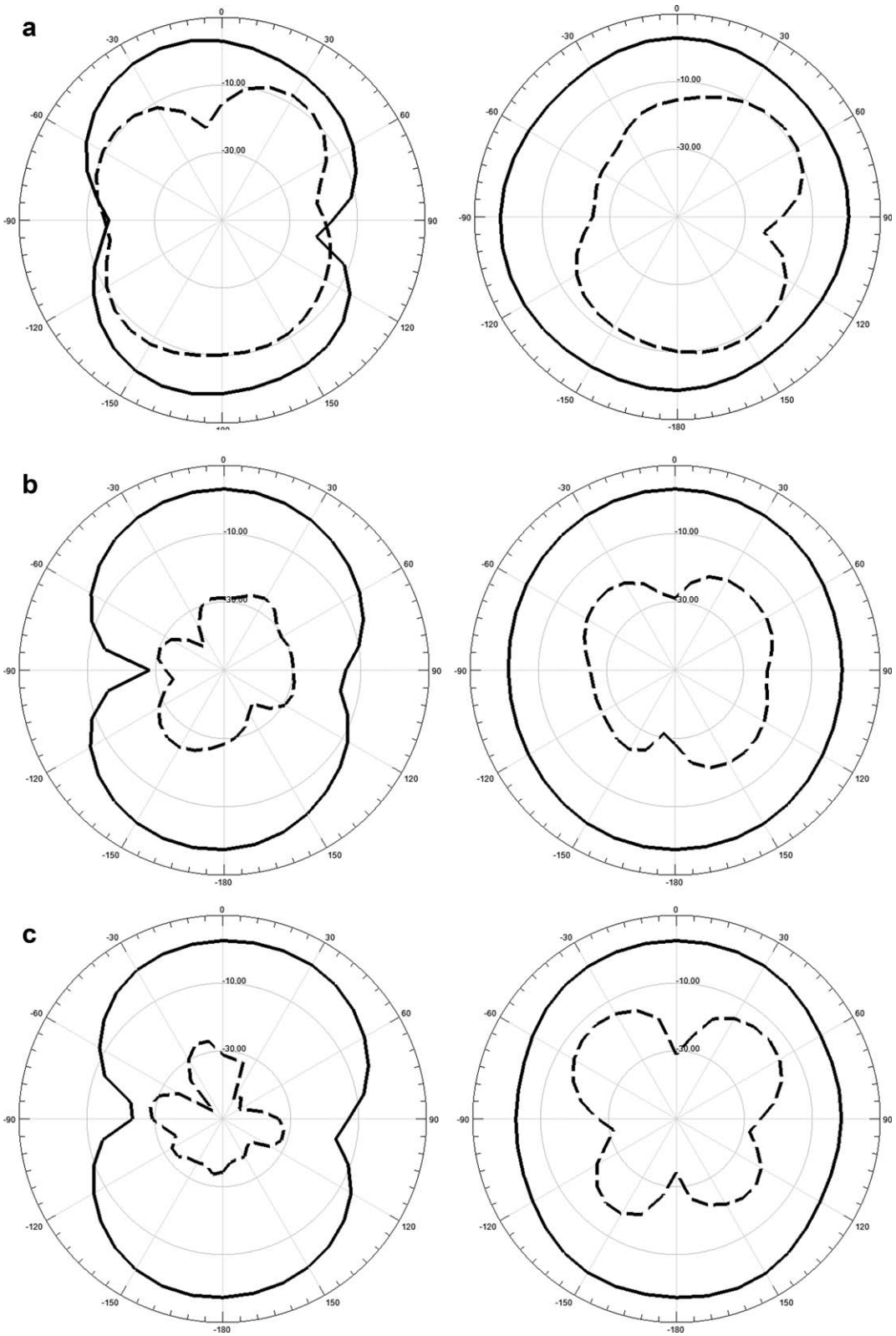

Figure 5 Far-field radiation patterns for the proposed antenna at (a) 4 GHz, (b) 6 GHz, (c) 7 GHz, and (d) 8 GHz

dimensions of the proposed antenna are as follows: $L1 = 6$ mm, $L2 = 11.5$ mm, $L3 = 1.5$ mm, $L4 = 1.5$ mm, $L5 = 9.5$ mm, $L6 = 6$ mm, $L7 = 1$ mm, $L8 = 6$ mm, $L9 = 3.5$ mm, $L10 = 12$ mm, $L11 = 2$ mm, $L12 = 1.5$ mm, $L13 = 1.5$ mm, $W1 = 22$ mm, $W2 = 6$ mm, $W3 = 5$ mm, $W4 = 3.2$ mm, $W5 = 5.5$ mm, $W6 = 6$ mm, $W7 = 1.5$ mm, $W8 = 1$ mm, $W9 = 6$ mm, $W10 = 8$ mm, $W11 = 6$ mm, and $W12 = 3$ mm. According to these parameters, the prototype of the proposed antenna is shown in Figure 2.

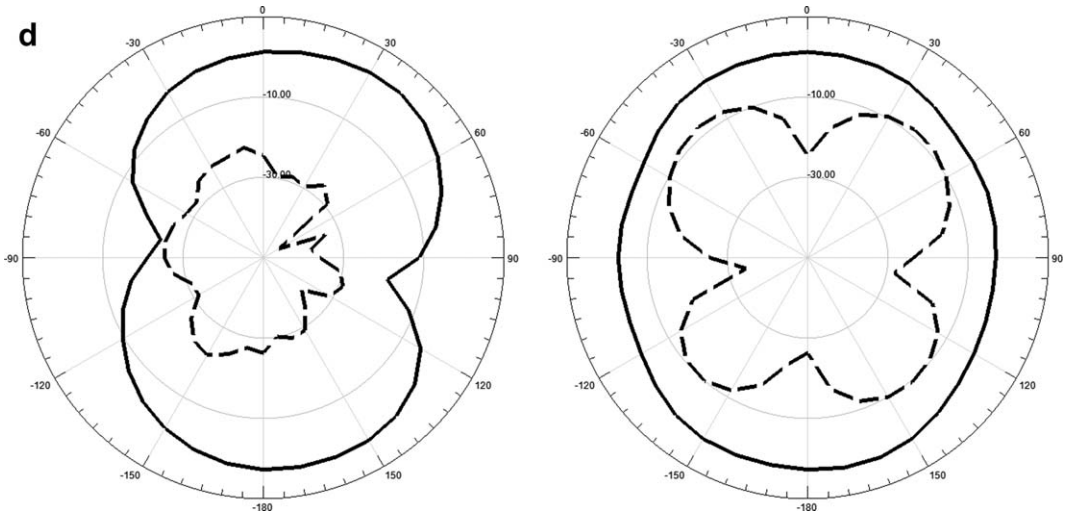

Figure 5 Continued

3. SIMULATION AND MEASUREMENT RESULTS

The proposed UWB antenna was constructed and simulated by using Ansoft HFSS software and the measurement was carried out by using Agilent N5244A vector network analyzer.

Figure 3 shows that the results of the simulation and the measurement agree with each other very well. The proposed antenna not only expands the bandwidth from 2.4 to 11.6 GHz (VSWR < 2), which is more than 131%, but also achieves the band-notched characteristic of the 3.3–3.8 GHz and 5.0–6.0 GHz by introducing the W-shaped slot in the monopole patch and the "6"-shaped resonance loop on the two sides of the feed line.

Figure 4 shows the simulated surface current distribution at 3.6 and 5.4 GHz, at the band notched frequency, the surface current distribution appears to be stronger around the W-shaped slot and the "6"-shaped resonance loop, so the radiation becomes weaker near the band-notched frequency.

Figure 5 shows the far-field radiation patterns at 4, 6, 7, and 8 GHz, the copolarization and cross-polarization in the x–z ($\phi = 0$) and y–z ($\phi = 90$) planes are given. It can be observed that the proposed antenna has an approximately omni-directional radiation patterns at these frequencies.

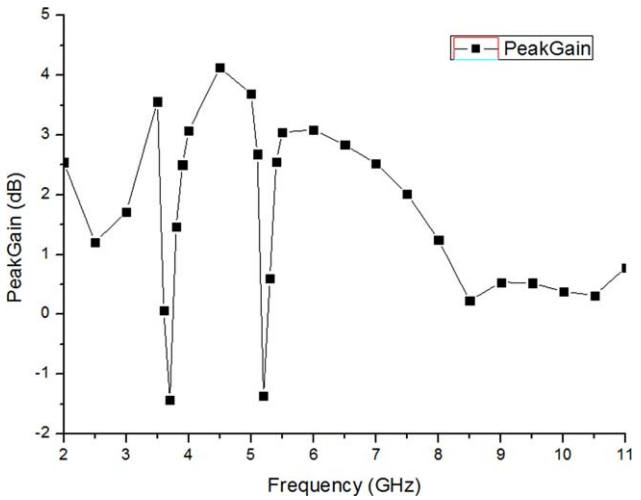

Figure 6 Peak gain of the proposed antenna against frequency

Figure 6 presents that the peak-gain of the proposed antenna has a sharp decrease at the band-notched frequency. In other frequencies outside the rejected band, the peak-gain can remain 0–4 dB.

4. CONCLUSION

A novel double band-notched antenna with nonequiwidth W-shaped slot and "6"-shaped resonance loop has been designed for UWB applications. By introducing W-shaped slot, the band-notched function can be obtained from 3.3 to 3.8 GHz and by introducing "6"-shaped resonance loop on the two sides of the feed line, the band-notched frequency at 5.0–6.0 GHz can be achieved. The results of the simulation and the measurement show that the impedance bandwidth can cover 2.4–11.6 GHz for VSWR < 2 (more than 131%) and nearly omni-directional radiation patterns in the whole bands and high gains except the notched frequency band. Therefore, the proposed antenna is suitable for UWB applications.

REFERENCES

1. H. Schantz, The art and science of ultrawideband antennas, Artec House, Norwood, 2005.
2. M. Ojaroudi, H. Ebrahimian, Ch. Ghobadi, and J. Nourinia, Small microstrip-fed printed monopole antenna for UWB application, Microwave Opt Technol Lett 52 (2010), 1756–1761.
3. X.-B. Sun and M.-Y. Cao. Wideband cpw-fed elliptical monopole antenna, Microwave Opt Technol Lett 52 (2010), 1774–1776.
4. G.-M. Zhang, J.S. Hong, B.-Z. Wang, Q.Y. Qin, J.B. Mo, and D.M. Wan, A novel multi-folded UWB antenna fed by CPW, J Electromagn Waves Appl 21 (2007), 2109–2119.
5. J. Liang, C.C. Chiau, X.D. Chen, and C.G. Parini, Study of a printed circular disc monopole antenna for UWB systems, IEEE Trans Antennas Propag 53 (2005), 3500–3504.
6. M. Naser-Moghadasi, R.A. Sadeghzadeh, M. Katouli, and B.S. Virdee, Ultra-wideband microstrip antenna with enhanced impedance bandwidth, Microwave Opt Technol Lett 52 (2010), 870–873.
7. A.A. Eldek, Numerical analysis of a small ultra-wideband microstrip-fed tap monopole antenna, Prog Electromagn Res (PIER) 66 (2006), 199–212.
8. S. Gao and A. Sambell, A simple broadband printed antenna, Prog Electromagn Res (PIER) 60 (2006), 119–130.
9. C.-W. Chiu and C.-S. Li, A cpw-fed band-notched slot antenna for UWB applications. Microwave Opt Technol Lett 51 (2009), 1587–1592.

10. S.-H. Choi, G.-T. Jeong, H.-H. Park, H.-C. Lee, and K.-S. Kwak, Compact band-notched ultrawideband Y-shaped antenna with dual inverted-L slots, Microwave Opt Technol Lett 50 (2008), 2797–2799.
11. X.-F. Zhu and D.-L. Su, Symmetric E-shaped slot for UWB antenna with band-notched characteristic. Microwave Opt Technol Lett 52 (2010), 1594–1597.
12. Q. Guo, Z. Li, J. Wang, and J. Ju, A band-notched cpw fed antenna with ring ground for ultra-wideband applications, Microwave Opt Technol Lett 52 (2010), 1691–1694.
13. J.-Y. Xue, S.-X. Gong, P. Fei, W. Wang, and F.-F. Zhang, Design of a compact ultrawideband slot antenna with dual band-notched function, Microwave Opt Technol Lett 53 (2011), 245–249.

DESIGN OF A PRINTED DIPOLE ARRAY ANTENNA WITH WIDEBAND POWER DIVIDER AND RF SWITCHES

Jhin-Fang Huang,[1] Jiun-Yu Wen,[2] and Wen-Cheng Lai[1]
[1] National Taiwan University of Science and Technology;
Corresponding author: jfhuang@mail.ntust.edu.tw
[2] National Communications Commission

Received 4 March 2013

ABSTRACT: *In this article, we use pattern-diversity technique to combine a RF single-pole double-throw (SPDT) switch with an antenna array together in order to reduce the signal distortion caused by multipath fading. In addition, in order to improve the way controlling the SPDT switch by software, a novel circuit structure which will control antenna pattern switching automatically by hardware is also developed. Return loss and radiation patterns are presented and compared with the measured results. Good agreement is achieved between computed and measured results and illustrates the validity of the designed method.*
 Microwave Opt Technol Lett 55:2410–2413, 2013; View this article online at wileyonlinelibrary.com. DOI 10.1002/mop.27858

Key words: *pattern diversity; dipole array antenna; RF switch*

1. INTRODUCTION

In recent years, wireless transceiver systems getting growth in the worldwide, improving resolution, speed and lowering power consumption and area of the circuit, become the most important issues [1–3]. Those reports are concerned only on components of antennas or RF IC integrated circuit designs. As commercial wireless communication systems generally require low-cost microwave components and antennas, here we combine them together to meet the low-cost demand.

Using radio-wave achievement to pass on the wave medium will meet some interference such as multipath and co-channel interference. In the indoor, the radio broadcast cannot avoid some effects which are caused by furniture, household appliances, and so on. If using traditional omnidirectional antennas as the space division multiple access for access point (AP) [4], the fading due to multipath and co-channel interference will be particularly serious; it also has the quite tremendous influence regarding the wireless transmission quality. Nowadays, in order to solve the interference problem for antenna, using the monopole antenna (its antenna gain is lower, *H*-plane is omnidirectional) with space diversity technology to reduce the multipath fading. Because of the antenna directivity is low and indoor environment goes to extremes complex, the signal attenuation is still unable completely to overcome. Furthermore, the gain of transmitted antenna is low, and the covered range is still small.

In this article, mostly discussion focuses on the user-end antenna improvement as well as the antenna design of WLAN interface card. Hence in this article, we will focus on the design of AP for WLAN. Using pattern-diversity [5,6] technique in the antenna system, also be called angular diversity, will reduce the signal distortion caused by multipath fading and improve the transmissibility. In addition, we improve the way controlling the single-pole double-throw (SPDT) switch by software, and develop a novel circuit structure controlling antenna pattern switching automatically by hardware.

2. FRONT-END SWITCHING CIRCUIT STRUCTURE

Figure 1 shows the traditional circuit of AP for WLAN. The traditional circuit of AP contains two SPDT switches and two omnidirectional antennas. The left side antenna is a half-duplex antenna port, serving as the transmitting-end or the receiving-end by controlling the switch SW1. The right side antenna is a simplex receiving antenna port. When the AP for WLAN in RX mode, the switch SW2 will choose an antenna whose received signal is stronger between two antennas as the receiving antenna; but it only uses the left side antenna in the TX mode. The features of both two antennas are low gain and omnidirectional antenna. The traditional antennas of AP for WLAN use the space-diversity technique. Space-diversity is a method of transmission or reception, in which the effects of fading are minimized by the simultaneous use of two or more separated antennas. In addition, the traditional circuit of AP must add a chip at internal front-end circuit to control the switch by software, then to achieve pattern-diversity function.

The novel antenna system includes Wilkinson power divider [7], RF SPDT switch, Schottky voltage multiplier, and D-flip-flop which is shown in Figure 2. In this circuit, voltage multiplier and D-flip-flop will be used to control SPDT switch variation automatically. A voltage multiplier is an electrical circuit that converts AC electric power from a lower voltage to a higher DC voltage; Schottky diode with a low forward voltage drop and a very fast switching action.

There are two modes for the working states of AP: RX and TX modes. RX mode: As shown in Figure 2, signals will be received by Ant 1 and Ant 2. In the RX mode, there is no signal at the inputs of voltage multiplier; the complementary outputs (Q and Q) of flip-flop will be logic 0 and 1. So the received signal by Ant 1 and Ant 2 will go through switch to postend processing circuit.

TX mode: Signals will be transmitted by postend processing circuit. In the meantime, postend processing circuit will also transmit RF signal to voltage multiplier; the produced DC voltage of voltage multiplier will set the input of D-flip-flop to

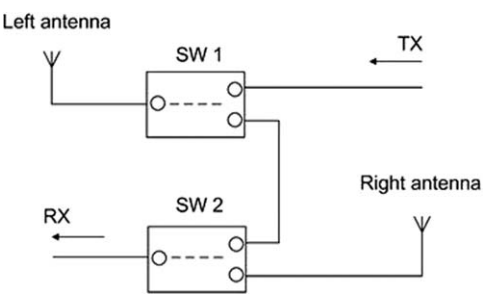

Figure 1 Traditional wireless AP internal circuit diagram